

## Formation and role of cool flames in plasma-assisted premixed combustion

W. Kim,<sup>a)</sup> M. G. Mungal, and M. A. Cappelli

Mechanical Engineering Department, Stanford University, Stanford, California 94305-3032, USA

(Received 13 November 2007; accepted 21 January 2008; published online 8 February 2008)

The structure of a plasma-assisted laminar premixed flame is studied numerically. The initial radical yield generated by a nonequilibrium discharge serves as the boundary condition for a one-dimensional flame code predicting the formation of a cool flame which pilots the premixed methane/air combustion. The ignition of the surrounding unactivated methane-air mixture by this cool flame is modeled as an opposed diffusion flame. Our findings indicate that the nonequilibrium discharge is an *in situ* reformer of the fuel for the production of the cool flame, producing primarily H<sub>2</sub> and CO, thus, facilitating the burning of the lean methane-air mixture. © 2008 American Institute of Physics. [DOI: 10.1063/1.2841894]

Plasma-based methods for enhancing premixed flame stability have emerged over the past two decades.<sup>1</sup> One such method employs a nonequilibrium ultrashort pulsed repetitive discharge (USRD) to greatly extend the flammability limit and to reduce ignition delay.<sup>2-4</sup> Previous studies<sup>5,6</sup> suggest that the discharge increases the flame speed, however, the precise mechanism by which combustion stability is enhanced is still not well understood. Measurements of a relatively low translational temperature ( $\sim 400$  K) in the vicinity of the pulsed nonequilibrium discharge suggests that thermal heating is not likely to be important in enhancing stability and others<sup>7-10</sup> have attributed the enhancement to the formation of excited species or radicals such as vibrationally hot molecular nitrogen (N<sub>2</sub>), as well as O, H, and ground-state and electronically excited OH (for the possible effects of thermal heating, see Refs. 2 and 10). The production of ground-state and electronically excited OH and OH\* partially explains the presence of intense OH band emission near the flame base of a plasma-assisted premixed flame.<sup>9-12</sup> However, recent experiments<sup>13</sup> in a lifted methane jet in crossflow air reveals that the discharge is separated from the flamebase by a distance that is too large for the survival of such short-lived ( $\sim 100$   $\mu$ s) radicals. The long discharge-to-flamebase distances seen in these experiments ( $\sim 1-10$  cm) indicate that the species produced in the plasma survive for relatively long periods ( $\sim 1-10$  ms) and that intermediate stable species are responsible for enhancing combustion.

In this letter, we present a numerical study that supports the conjecture that the nonequilibrium discharge that we have used in stabilizing premixed flames<sup>11</sup> gives rise to conditions very similar to that of so-called cool flames<sup>14</sup>—i.e., premixed flows of sustained low temperature partial oxidation and reforming reactions, forming species such as H<sub>2</sub> and CO, that enhance combustion. The simulations are facilitated by initial yield calculations for a pulsed discharge as carried out by Penetrante *et al.*,<sup>15</sup> coupled to a one-dimensional (1D) flame calculation, PREMIX,<sup>16</sup> to simulate the production and evolution of discharge initiated radicals within a premixed stream tube passing through the discharge. In the evolution of this stream following discharge activation, we confirm that low temperature ( $\sim 600$  K) partial oxidation reactions occur to produce H<sub>2</sub> and CO. In the flow configuration de-

scribed below, these species diffuse into premixed regions of the flow that are not activated by the discharge, promoting flame ignition and stabilization. To simulate this interaction, we treat this downstream structure as an opposed jet diffusion flame [using the simulation OPPDIF (Ref. 16)], with the stream flow velocity and mole fractions computed by the 1D premixed calculation used as a boundary condition. This later stage of the simulation captures the extension of the lean flammability limit of the flame,<sup>11</sup> which we find to be dependent strongly on the H<sub>2</sub> and CO generated in the plasma-activated cool flamelike stream.

A photograph of the USRD plasma-enhanced premixed methane/air flame that motivated this simulation is shown in Fig. 1. The equivalence ratio ( $\phi$ ) of the mixture is 0.53, which is below the lean flammability limit of methane ( $\phi_{LF}=0.55$ ). The premixed methane/air jet flows through a hollow quartz cylindrical section and a small portion of it passes through the pulsed discharge sustained between two electrodes, as shown. The visible discharge/flame is always biased to the cathode region due to the force generated by the ion wind. From the flow trajectory in the figure, we find that the ion wind dominates flow inertia (with  $\sim 1$  m/s flow speed) in the vicinity (within  $\sim 3$  mm downstream) of the discharge and diminishes further downstream. The intense luminous spot in Fig. 1 is the discharge kernel and just downstream of this is a region of diffuse, blue-white emission, which we will refer to here as the cool flame, dominated primarily by the characteristic  $A^2\Sigma^+ \rightarrow X^2\Pi$  electronic transition in OH at approximately 309 nm.<sup>11</sup> Surrounding this cool flame is a relatively strong blue emission associated with the  $A^2\Delta \rightarrow X^2\Pi$  electronic transition in CH at approxi-

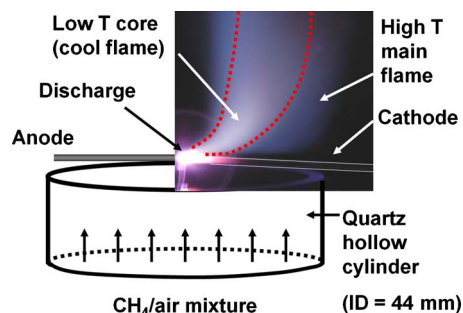


FIG. 1. (Color online) USRD assisted methane/air premixed flame. The red dotted lines represent the visible boundary of the cool flame.

<sup>a)</sup>Electronic mail: wkkim@stanford.edu.

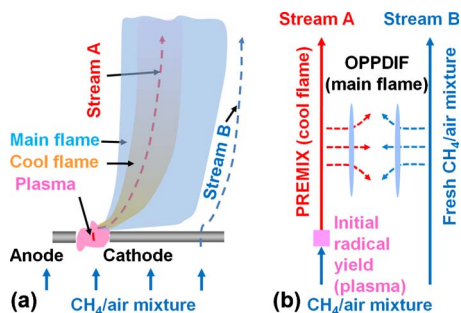


FIG. 2. (Color online) (a) A schematic interpretation of the flame structure and (b) corresponding geometry considered for the numerical simulation.

mately 430 nm, indicative of the presence of a high temperature flame sheet, typical of what is seen in premixed methane-air combustion. Abel inversion of the OH emission in this postdischarge region (22 mm downstream of the discharge to avoid the region of departure from an axisymmetric flow) indicates that the cool flame is volume filling, i.e., not a flame sheet in the usual sense. At lower equivalence ratios, the cool flame is present without the ignition of the surrounding high temperature flame. Under these conditions, this cool flame region can be probed with a simple thermometer, and its temperature is found to be very low ( $<500$  K).

A qualitative interpretation of the discharged-enhanced flame structure is depicted in Fig. 2(a), and the geometry considered for the simulation is shown in Fig. 2(b). As described above, the present simulations combine three calculations: (i) the determination of the initial radical yields (and hence radical flux) due to the discharge exciting a portion of the flow; (ii) a 1D reacting flow calculation along the streamwise direction [along the red line drawn in Fig. 2(a)] to simulate the formation of the cool flame [brown colored region in Fig. 2(a)] and (iii) a quasi-1D opposed flame simulation to capture the interaction between this activated stream and the surrounding nonactivated premix stream transverse to the streamwise directions. We recognize that this simulation is not an exact representation of the flow field, but only a first approximate attempt at understanding the flame structure prior to carrying out two-dimensional (2D) or three-dimensional simulations of the complex flow field.

The initial radical yield calculation is determined from a solution of the Boltzmann equation [using the commercially available Boltzmann solver, *BOLSIG* (Ref. 17)] for the discharge electron energy distribution function (EEDF) assuming a reduced electric field (electric field to mixture number density ratio) of  $E/n=300$  Td estimated from the discharge peak voltage, pressure, and electrode separation typical of that used in our experiments (6 kV, 1 atm, and 1 mm, respectively). Only initial parent species present in the mixture, i.e., nitrogen, oxygen, and methane ( $N_2, O_2, CH_4$ ), are assumed to affect the EEDF, over the time scales of the voltage pulses (15 ns). The resulting EEDF is used to determine the reaction rate constants for the following three electron-impact dissociation reactions considered,  $CH_4+e\rightarrow CH_3+H+e$ ,  $N_2+e\rightarrow 2N+e$  and  $O_2+e\rightarrow 2O+e$ . Following Penetrante *et al.*,<sup>15</sup> initial radical yields are computed using the average discharge power (10 W at 15 kHz pulse repetition rate). The initial concentration of these radicals and their parent species ( $CH_4$  and air) are determined from the known equivalence ratios (0.53 and 0.49 for the cases studied here), pressure (1 atm), flow temperature (400 K, as measured in

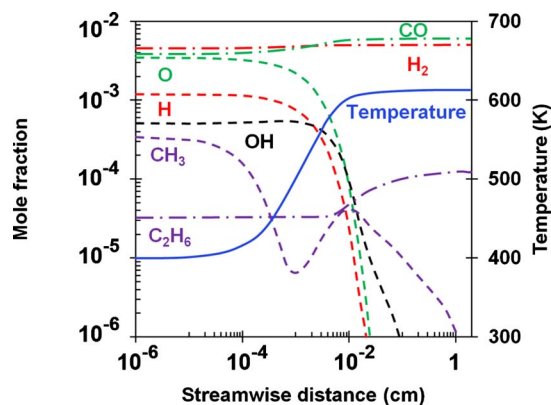


FIG. 3. (Color online) Temperature and representative species concentration profiles along the cool flame. Equivalence ratio is 0.53.

the discharge kernel in Ref. 18), flow velocity (1 m/s,  $Re_d = \sim 1700$ ), and effective plasma area (1 mm<sup>2</sup>). The two specific equivalence ratios were selected because they straddle the lean flammability limit of the discharge-sustained flame, i.e., it is found that with the plasma activation, the main flame will extinguish at an equivalence value between these two cases.<sup>11</sup> The resulting concentrations and temperature from this calculation are used as initial conditions to the 1D PREMIX simulation.

The PREMIX simulation, using the GRI MECH 3.0 chemical kinetics mechanism,<sup>19</sup> serves to determine the structure of the cool flame as it evolves along the direction (labeled as stream A) shown in Fig. 2(b). The products of this activated stream mix with the unactivated stream [stream B in Fig. 2(b)] serve to promote ignition of the ultralean mixture. Conditions for the activated stream of the OPPDIF simulation are determined by the computed PREMIX products of the activated stream at a location 1 mm above the discharge. The 1 mm height is a representative location of the cool flame far field ( $>0.1$  mm), where a quasisteady state has been achieved (see Fig. 3). The nonactivated stream of the OPPDIF simulation is taken as the properties of the methane/air mixture that bypasses the discharge (1 atm, 300 K temperature). The separation between the two streams is chosen to be 1 cm in accordance with the transverse flame length scale of the experiments and the initial speed of both streams are taken to be 1.5 m/s to achieve a local 2D principal strain rate (maximum eigenvalue of the 2D strain rate tensor) of  $485$  s<sup>-1</sup> in the high temperature flame zone, close to that expected for a typical premixed flame ( $\sim 500$ s<sup>-1</sup>).<sup>20</sup> As expected, the simulated flame extinction limit is found to be somewhat sensitive to this strain rate.

The calculated evolution in temperature and mole fraction of representative species along the discharge-activated stream for an equivalence ratio of  $\phi=0.53$  are shown in Fig. 3. We see that the rapid recombination (within 0.1 mm) of radicals initially formed in the discharge (H, CH<sub>3</sub>, N, and O), result in a mild temperature increase ( $\sim 200$  K), and the formation of more stable intermediate species such as H<sub>2</sub>, CO, and C<sub>2</sub>H<sub>6</sub>. These stable species seem to persist for the duration of the PREMIX simulation (2 cm, or approximately 20 ms in time), suggesting that the cool flame contains partially oxidized and reformed fuel produced from the initial radicals formed in the discharge.

The computed temperature and CH mole fraction, the latter of which is an indicator of the flame reaction zone,

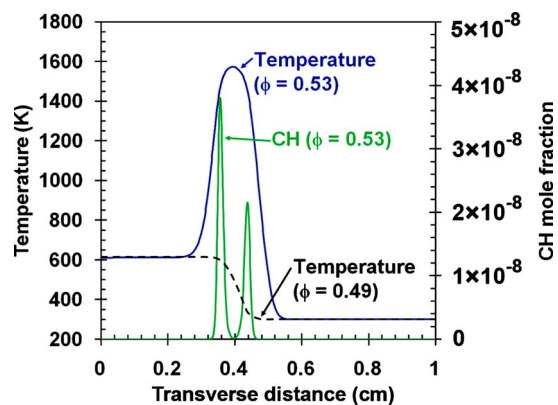


FIG. 4. (Color online) Temperature and CH profiles along the transverse direction. The CH peak represents the expected location of the high temperature flames.

along the transverse direction from the opposed jet diffusion flame simulations for both the  $\phi=0.53$  and  $\phi=0.49$  cases are shown in Fig. 4. We see that for  $\phi=0.53$ , there is a significant temperature increase ( $\sim 1600$  K) concomitant with combustion. We also see that with  $\phi=0.49$ , there is no flame, consistent with the flammability limit obtained in our previous experiments.<sup>11</sup> It is also noteworthy that when ignited, the simulation predicts a dual-flame structure, where the combustion of the outer unactivated stream is stabilized by the combustion products of the inner discharge-stabilized stream.

A pseudosensitivity analysis was carried out to better understand the role played by individual species generated in the cool flame, on the ignition and stabilization of the premixed flame. Species formed in the PREMIX simulation phase were individually removed from the activated stream (and mole fractions renormalized) that is introduced into the OPPDIF simulation phase, and the stream initial temperature was adjusted to identify the minimum temperature needed for flame ignition. The results of this analysis indicate that both  $H_2$  and CO have the greatest propensity for maintaining ignition, and the removal of either one of these species from the cool flame products results in flame extinction at approximately 600 K. In contrast, the removal of any other species (but keeping both  $H_2$  and CO in the cool flame) results in extinction at much lower temperatures ( $\sim 550$  K).

It is noteworthy that  $H_2$  and CO are the major products of conventional fuel reforming processes.<sup>21</sup> The findings from our simulation, and the above sensitivity analysis indicates that our nonequilibrium discharge seems to serve as the initial radical source for an *in situ* reformer of the fuel, and not a direct radical source for combustion enhancement, which is contrary to the conventional wisdom shared in the plasma-assisted combustion literature.<sup>7-11</sup> The cool flame, in which the fuel reforming takes place, pilots the combustion

of the surrounding lean fuel-air mixture, greatly extending the lean flammability limit. Future studies will focus on the detection of  $H_2$  and CO in this postdischarge region, and in confirming the presence of this dual flame structure shown in Fig. 4.

This work was sponsored by the AFOSR/MURI Program—Experimental/Computational Studies of Combined-Cycle Propulsion: Physics and Transient Phenomena in Inlets and Scramjet Combustors, a joint effort of the University of Texas at Austin and Stanford University, with Julian Tishkoff as the Technical Monitor.

- <sup>1</sup>S. M. Starikovskaia, J. Phys. D **39**, R265 (2006).
- <sup>2</sup>A. Bao, Y. G. Utkin, S. Keshav, G. Lou, and I. V. Adamovich, IEEE Trans. Plasma Sci. **35**, 1628 (2007).
- <sup>3</sup>S. V. Pancheshnyi, D. A. Lacoste, A. Bourdon, and C. O. Laux, IEEE Trans. Plasma Sci. **34**, 2478 (2006).
- <sup>4</sup>S. A. Bozhenkov, S. M. Starikovskaia, and A. Yu. Starikovskii, Combust. Flame **133**, 133 (2003).
- <sup>5</sup>Y. Ju, S. O. Macheret, M. N. Shneider, R. B. Miles, and D. J. Sullivan, 40th AIAA/ASME/SAE/ASEE Joint Propulsion Conference and Exhibit, Fort Lauderdale, FL, 2004 (unpublished), Paper No. 2004-3707.
- <sup>6</sup>I. I. Esakov, L. P. Grachev, K. V. Khodataev, V. A. Vinogradov, and D. M. Van Wie, IEEE Trans. Plasma Sci. **34**, 2497 (2006).
- <sup>7</sup>A. Yu. Starikovskii, Proc. Combust. Inst. **30**, 2405 (2005).
- <sup>8</sup>N. Chintala, A. Bao, G. Lou, and I. V. Adamovich, Combust. Flame **144**, 744 (2006).
- <sup>9</sup>J. Liu, F. Wang, G. Li, A. Kuthi, E. J. Gutmark, P. D. Ronney, and M. A. Gundersen, IEEE Trans. Plasma Sci. **33**, 326 (2005).
- <sup>10</sup>G. P. Pilla, D. A. Galley, D. A. Lacoste, F. Lacas, D. Veynante, and C. O. Laux, IEEE Trans. Plasma Sci. **34**, 2471 (2006).
- <sup>11</sup>W. Kim, H. Do, M. G. Mungal, and M. A. Cappelli, Proc. Combust. Inst. **31**, 3319 (2007).
- <sup>12</sup>E. I. Mintoussov, A. A. Nikipelov, S. S. Starikovskaia, and A. Yu. Starikovskii, 44th AIAA Aerospace Sciences Meeting and Exhibit, Reno, NV, 2006 (unpublished), Paper No. 2006-614.
- <sup>13</sup>W. Kim, H. Do, M. G. Mungal, and M. A. Cappelli, Combust. Flame (accepted).
- <sup>14</sup>A. Fish, Angew. Chem., Int. Ed. Engl. **7**, 45 (1968).
- <sup>15</sup>B. M. Penetrante, M. C. Hsiao, B. T. Merritt, G. E. Vogtlin, P. H. Wallman, M. Neiger, O. Wolf, T. Hammer, and S. Broer, Appl. Phys. Lett. **68**, 3719 (1996).
- <sup>16</sup>R. J. Kee, F. M. Rupley, J. A. Miller, M. E. Coltrin, J. F. Grcar, E. Meeks, H. K. Moffat, A. E. Lutz, G. Dixon-Lewis, M. D. Smooke, J. Warnatz, G. H. Evans, R. S. Larson, R. E. Mitchell, L. R. Petzold, W. C. Reynolds, M. Caracotsios, W. E. Stewart, and P. Glarborg, Chemkin Collection, Release 4.0, Reaction Design, Inc., San Diego, CA (<http://www.reactiondesign.com/>).
- <sup>17</sup>J.-P. Boeuf, L. C. Pitchford, and W. L. Morgan, SIGLO-KINEMA Software, Monument, CO (<http://www.siglo-kinema.com/bolsig.htm>).
- <sup>18</sup>W. Kim, H. Do, M. G. Mungal, and M. A. Cappelli, IEEE Trans. Plasma Sci. **34**, 2545 (2006).
- <sup>19</sup>G. P. Smith, D. M. Golden, M. Frenklach, N. W. Moriarty, B. Eiteneer, M. Goldenberg, C. T. Bowman, R. K. Hanson, S. Song, W. C. Gardiner, Jr., V. V. Lissianski, and Z. Qin ([http://www.me.berkeley.edu/gri\\_mech](http://www.me.berkeley.edu/gri_mech)).
- <sup>20</sup>M. G. Mungal, L. M. Lourenco, and A. Krothapalli, Combust. Sci. Technol. **106**, 239 (1995).
- <sup>21</sup>C. Higman and M. J. van der Burgt, *Gasification* (Elsevier Science, Burlington, 2003), p. 1.